Article

Mechanical Properties and Tribological Behavior of MoS$_2$-Enhanced Cellulose-Based Biocomposites for Food Packaging

Shih-Chen Shi [1,*] [ID]**, Pramod Kumar Mandal** [1] **and Tao-Hsing Chen** [2,*] [ID]

[1] Department of Mechanical Engineering, National Cheng Kung University (NCKU), No. 1 University Road, Tainan 70101, Taiwan; n16047151@mail.ncku.edu.tw

[2] Department of Mechanical Engineering, National Kaohsiung University of Science and Technology, Kaohsiung 80778, Taiwan

* Correspondence: scshi@mail.ncku.edu.tw (S.-C.S.); thchen@nkust.edu.tw (T.-H.C.)

Abstract: Synthetic polymers are the most commonly used polymers in daily life. Therefore, it is necessary to develop environmentally friendly polymers. Hydroxypropyl methylcellulose (HPMC) is a potential candidate for a biopolymer, owing to its unique properties. However, HPMC biopolymers have some disadvantages compared to synthetic polymers. In this study, the mechanical properties and tribological performance of MoS$_2$ additive-enhanced cellulose matrix biocomposites were investigated in order to improve the properties of HPMC. MoS$_2$ was incorporated into the HPMC matrix as a strengthening additive. The mechanical properties, bonding, and water vapor permeability of the composites were analyzed. The mechanical and vapor barrier properties of the HPMC films were significantly enhanced. The ultimate tensile strength and Young's modulus of the composite films increased with the addition of up to 1 wt% MoS$_2$. The water vapor permeability of HPMC films reduced when additives were incorporated. The wear test proves that the MoS$_2$ additives can improve the tribological performance of the HPMC composite while reducing the friction coefficient. The main reason for enhanced tribological performance is the improvement in load capacity of the composite coating by the MoS$_2$ additive. This MoS$_2$/HPMC biocomposite can be used in food packaging.

Keywords: cellulose; MoS$_2$; mechanical properties; water vapor permeability; tribology

1. Introduction

When food is exposed directly to air, it is not contaminated by dust easily but becomes more likely to breed bacteria and other microorganisms, which may cause diseases. Food packaging can block direct contact with air, moisture, and light and can prevent contamination during transportation and sale, thereby extending shelf life and making the food safer and more hygienic. Since the development of food packaging in response to urban development and the needs of people's lives, it has also become necessary to consider the convenience and efficiency of food management in a large number of transport, handling, storage, sales, and eating cases. The advantages of traditional plastic packaging are its low price, low density, toughness, ease of production, and low water vapor permeability. However, the development of new food packaging materials is necessary due to ecological demands. Moreover, a food packaging material must ensure freshness, safety, and environmental protection. Some studies have employed nanotechnology and decomposable materials for food packaging [1,2]. The basic need of future food packaging materials is decomposable materials, bio-friendly materials, low light penetration, excellent gas/moisture barrier properties, and appropriate mechanical properties. At present, the common materials that meet the above requirements are cellulose [3–5] and chitosan [6–8].

Chemically modified polymers have been extensively investigated for the development of new biomaterials with excellent physicochemical properties. Cellulose is the most

abundant polysaccharide found in nature. It is regular and linear and has a rigid structure because of its configuration and intramolecular hydrogen bonds. The intermolecular hydrogen bonds between the hydroxyl groups result in aggregates or crystalline forms of cellulose. This association between the molecules leads to the formation of highly ordered crystalline regions, which makes cellulose only slightly soluble in pure water [9].

Synthetic polymers are the most used polymers in daily life. However, they are non-biodegradable, difficult to recycle, and based on non-renewable materials. Therefore, the development of environmentally friendly and biodegradable polymers of natural origin that can replace synthetic polymers is necessary for environmental and resource conservation. Hydroxypropyl methylcellulose (HPMC) is an odorless and tasteless edible plant derivative with properties such as transparency, oil resistance, and the ability to form a gel upon heating. Considerable work has been conducted on the characteristics of HPMC, which possesses unique tribological properties [10], self-healing behavior [11], and features that are amenable to enhancement [12]. Furthermore, HPMC can be easily detected using standard analytical tools, which are suitable for industrial applications. However, HPMC biopolymers have some disadvantages compared to synthetic polymers such as poor tensile strength, elongation factor, and water vapor barrier performance. As a result of these disadvantages, they cannot be used in practical applications. Consequently, several studies have used additives to improve the properties of HPMC [13,14]. This study investigates the effects of molybdenum disulfide (MoS_2) additives on mechanical properties and tribological behavior.

MoS_2 has a low friction coefficient. When added to polymers, it forms composites with improved strength and reduced friction. Previous studies have demonstrated the use of MoS_2 additives in applications, such as lubrication, anti-wear, anticorrosion [15], and biocompatibility [16].

The addition of appropriate quantities of MoS_2 can enhance the tribological performance of HPMC, and the mechanism responsible for this is well-understood; MoS_2 and HPMC will peel off from the coating surface to form a transfer layer [17]. However, the effects of additives on the mechanical properties of composite films and the relationship between these mechanical properties and tribological performance are unknown.

HPMC has potential for applications in food packaging [18,19], pediatric usage [20], and drug release control techniques [21]. Thus, analyzing the mechanical and tribological properties of HPMC films is significant. Therefore, we studied the mechanical properties of HPMC polymer films with different molecular masses, the augmentative effects of MoS_2 addition, and their mechanisms. In addition, the factors that influence the water vapor permeability (WVP) of the composite films are discussed. The findings of this study can serve as a useful reference for the diversification of HPMC film applications.

2. Materials and Methods

2.1. Materials

Hydroxypropyl methylcellulose (HPMC, Pharmacoat 645, 606, and 615, Shin-Etsu, Tokyo, Japan) of three grades based on viscosity and molecular weight as shown in Table 1 was used. MoS_2 particles with an average size of 2 μm were obtained from Sigma Aldrich (St. Louis, MO, USA). The material properties of HPMC and MoS_2 are listed in Table 2.

Table 1. Specifications of hydroxypropyl methylcellulose (HPMC) powders.

Grade	Molecular Weight (g/mol)	Viscosity (mPas)
HPMC 645	20,000	4.5
HPMC 606	35,600	6
HPMC 615	60,000	15

Table 2. Material properties of HPMC and MoS_2.

Material	Degradability	Biofriendly	Light Absorption	Moisture Barrier	Strength	Tribology Properties
HPMC	Good [22]	Good [23]	Bad	Bad	Bad	Bad
MoS_2	Bad	Good [16]	Good [24]	Good [25]	Good [26]	Good [27]

2.2. Film Preparation

The preparation of MoS_2/HPMC composite films followed a four-step process. Initially, water and ethanol were mixed in a ratio of 1:4 in a clean flask and then heated to 60 °C. Then, 3 g of all grades of HPMC powder was poured into the solvent of 100 g and magnetically stirred at 500 rotations per minute for 12 h. Then, MoS_2 additives (listed in Table 3) were added to HPMC solution. After preparation, the solution was stilled for 3 h for degassing and in order to prevent the formation of microbubbles within the films. A 30 g mixture MoS_2/HPMC solution was then poured into a petri dish for film preparation and placed inside a controlled-environment chamber at $40 \pm 10\%$ relative humidity (RH) and at 30 ± 10 °C to dry the film. After 6 h, the petri dish was removed from the chamber, placed at a temperature of 25 °C with a relative humidity of 60%, and dried for 24 h. After drying, the films were removed from the Petri dish and stored under 30% RH at 25 °C. Both film thickness and surface roughness (Ra) were measured using a 3D laser scanning microscope (VK9700, Keyence, Osaka, Japan), controlled at 200 ± 10 μm and 2 ± 0.5 μm. A scanning electron microscope (SEM, AURIGA, Carl Zeiss AG, Jena, Germany) was used to observe the surface morphology of the coating.

Table 3. Masses of nanoparticle additives used in film and corresponding percent by weight concentration.

MoS_2 (g)	0	1.03	2.06	3.09	5.15
MoS_2 (wt%)	0	1	2	3	5

2.3. Determination of Mechanical Properties

The cast films were removed and cut into a bone shape using an ASTM D-638-V "dog bone" punch. Films with cracks, nicked sides, or bubbles were discarded. The mechanical properties of the cast films were determined using a micro/nano tensile testing machine (DDS32, Kammrath & Weiss GmbH, 44,141 Dortmund, Germany) according to the ASTM D882 standard.

2.4. Material Properties Analysis of Composite

The crystallization parameters were collected by a Bruker D2 Phaser diffractometer, using CuKα (Kα1, 0.15406 nm) at an operating voltage and current of 30 kV and 10 mA, respectively. The blank scan was carried out using a clean zero background plate with no applied sample. The blank scan was subtracted from the sample scan during the analysis. The intermolecular force was determined using attenuated total reflection (ATR) Fourier transform infrared (FTIR) spectroscopy (Thermo Nicolet NEXUS 470, Golden Valley, MN, USA, GMI). The WVP of films was measured according to the ASTM 1290-93 standard [28]. A unique glass cup with a diameter of 6.5 cm and a depth of 3.5 cm, with a small platform at the top to seal the films, was used to assess the WVP of the prepared films. The films were cut into discs with a diameter slightly larger than that of the cup. Distilled water (10 mL) was dispensed into the cup, which was then covered with the film and sealed with a ring. The cup was weighed and placed inside a controlled environment chamber at 30 °C and ± 40 RH. The cups were weighed every 8 h to obtain at least four data points. The WVP of the film was calculated using the following equation:

$$WVP = (WVTR \cdot y)/(p_1 - p_2), \tag{1}$$

where y is the mean thickness of the film, and p_1 and p_2 are the partial pressures of water vapor on the lower and upper side of the film, respectively.

Water vapor transmission rate (WVTR) was in turn obtained as follows:

$$WVTR = weight\ loss\ per\ unit\ time/film\ area. \tag{2}$$

2.5. Tribology Performance of MoS₂/HPMC Composite Film

The tribological performance was evaluated using a ball-on-disk tribometer (POD–FM406–10NT, Fu Li Fong Precision Machine, Kaohsiung, Taiwan) under a load of 2 N and disk speed of 0.03 m/s. A chrome steel ball (52,100 steel) with a diameter of 6.31 mm was employed as the upper ball, and the composite films were employed as the lower disk test piece. The wear test was performed in an environment at 25 °C and a RH of 70%. The friction coefficient of the coating was monitored and recorded in real time, and the wear volume was measured using a 3D laser scanning microscope.

2.6. Third-Body Theory

The third-body theory describes the interaction of the counterpart of the materials involved in the abrasion dry friction conditions [29,30]. The velocity accommodation mechanism refers to the location and motion state of the wear as sites (S) and modes (M). S1 and S5 are called the first-bodies (representing two counter-wear parts); S3 refers to the natural wear debris generated by abrasion or lubricant additive; and S2 and S4 are the interface layers between S1, S3, and S5–S3. Mode represents the mode of velocity accommodation. M1–M4 represent elastic deformation, normal breaking/rupture, hearing/sliding, and rolling mechanisms, respectively [31].

3. Results and Discussion

3.1. Surface Morphology and XRD Analysis of Composite Film

The SEM image showing the surface pattern of the MoS₂ 1 wt%/HPMC composite is presented in Figure 1a. The image shows that the additive and HPMC matrix are in good condition and that there is no obvious particle agglomeration. Figure 1b shows the micro/nano tensile testing sample made of the MoS₂ 1 wt%/HPMC composite. The composite material is black in color, which means that the addition of MoS₂ turns the originally transparent HPMC into black and can absorb a large amount of light, achieving the purpose of blocking light. The tribological behavior of MoS₂ is immensely sensitive to environmental conditions. In extremely humid environments, sulfides are prone to combination with the moisture in air and form oxides, resulting in a decrease in tribological performance [32]. Meanwhile, the structure and morphology of MoS₂ affect its abrasive performance [33]. Therefore, it is crucial to understand the structure of MoS₂ additives in composite materials following the preparation process. The above samples were analyzed via X-ray diffraction (XRD) analysis, and the results are shown in Figure 1c. XRD patterns of the MoS₂/HPMC composite are shown in Figure 1. The MoS₂/HPMC composite clearly displays diffraction peaks of MoS₂, which can be indexed to the (002), (004), (100), (103), (006), (105), and (110) planes of 2H-MoS₂ (JCPDS card No. 37-1492). This result indicates that the preparation process does not damage the 2H-MoS₂ additives. Meanwhile, the highly intense (002) peak indicates that the layered structure of MoS₂ is parallel to the composite surface, which helps to discern its tribological properties.
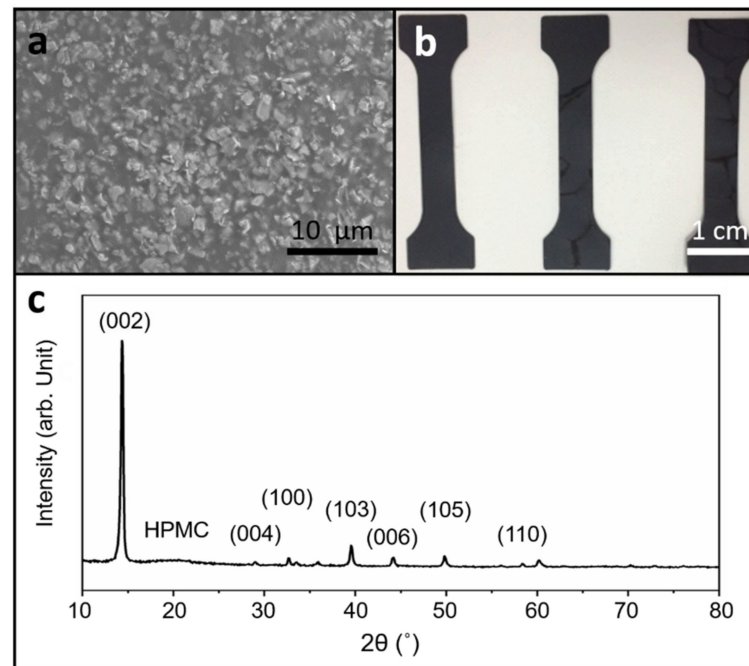
Figure 1. (**a**) SEM image of composite film; (**b**) samples for micro-tensile test; and (**c**) XRD analysis results of MoS$_2$/HPMC composite.

3.2. Mechanical Properties of Composite Films

　　The tensile strength, elastic modulus, and percentage elongation of the films were measured to evaluate the improvements in the mechanical properties of composite films compared to those of pure HPMC. The stress–strain curves of the composite films with three different molecular masses (molecular chain lengths) are shown in Figure 2. HPMC with longer molecular chains exhibited better mechanical properties. The addition of small quantities (1%) of MoS$_2$ additives enhanced the ultimate tensile strength (UTS) of the film but reduced its ductility. Furthermore, as the amount of MoS$_2$ increased, UTS and ductility of the film decreased. This may be because an appropriate amount of additive could form better local bonding with the HPMC matrix. This hypothesis can be verified with the experimental results of FTIR.
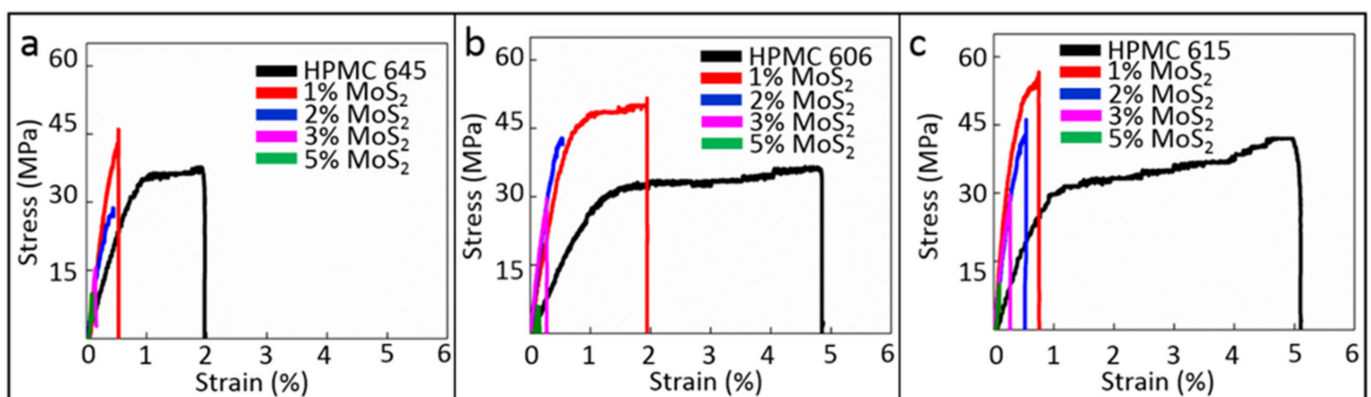

Figure 2. Nano-tensile tester results of the (**a**) MoS$_2$/HPMC 645, (**b**) MoS$_2$/HPMC 606, and (**c**) MoS$_2$/HPMC 615 composites.

　　Figure 3 shows that the addition of 1 wt% of MoS$_2$ provided the best result in terms of UTS, that is, an increase of up to 20%. A further increase in MoS$_2$ additives led to a significant decrease in UTS. As shown in Figure 4, the elastic modulus of the MoS$_2$/HPMC composite considerably improved when the amount of additive was less than 3%, sug-

gesting that the elastic behavior of the films was strongly affected by a small amount of additives. The elastic moduli of the films containing 1–3% MoS_2 were dramatically more significant than those of the pure HPMC matrix from 1500 to 30%. Therefore, the addition of MoS_2 within this range improved the matrix bonding. Based on the elongation (EL) analysis shown in Figure 5, the addition of MoS_2 embrittled HPMC films and changed these films from ductile to brittle materials. Shi et al. [27] found that the addition of 5–10% MoS_2 resulted in optimal tribological properties. This is due to the fact that the primary mechanical property in this study is tensile strength, whereas wear and lubrication occur under compressive conditions. As the addition of MoS_2 particles embrittled an HPMC film, the material broke down when subjected to stress, allowing the MoS_2 particles to directly contact the wear component. Hence, the attainment of optimal wear resistance and friction coefficients at higher additive ratios (5–10%) was caused by the combination of material breakage with various accommodation mode tribological mechanisms of MoS_2 [12,34] and the ease with which MoS_2 synergizes with HPMC to form the transfer layers. However, the breakdown of the material also accelerated film depletion. This is consistent with previous findings, which have reported that the addition of MoS_2 cannot extend the service life of a film [17].
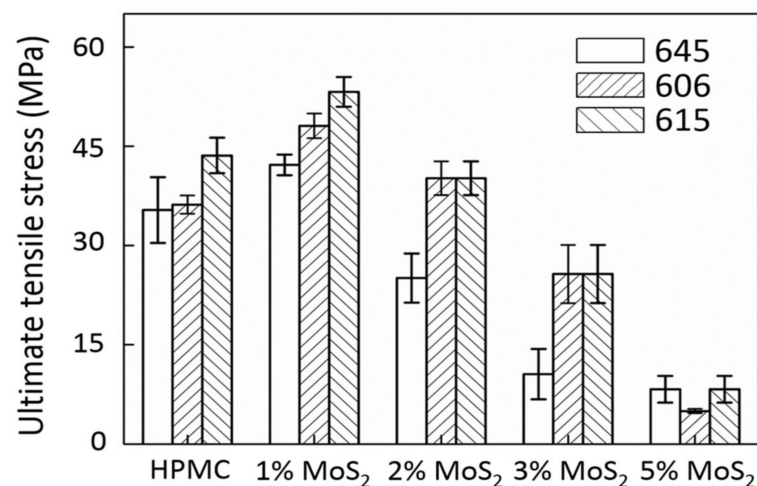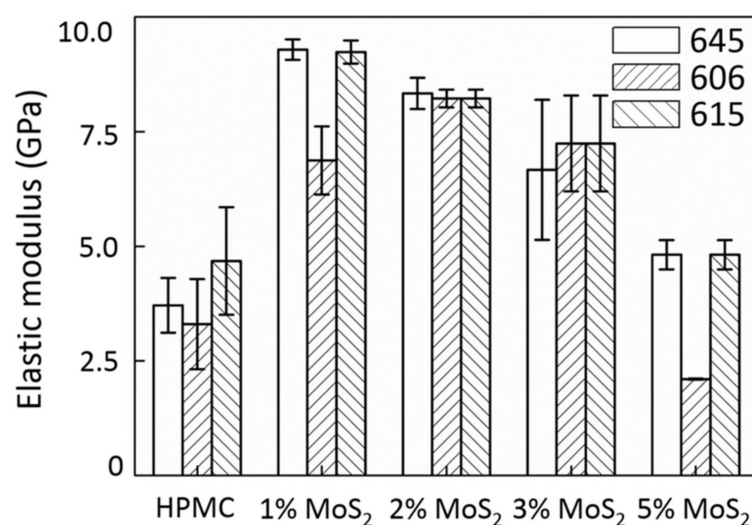

Figure 3. UTS results of MoS_2/HPMC composites.

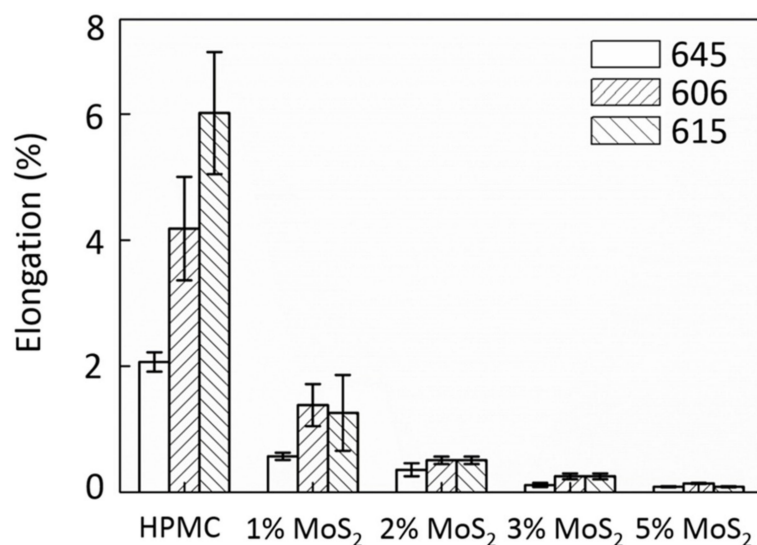**Figure 4.** Elastic modulus of MoS_2/HPMC composites.

Figure 5. Elongation of MoS_2/HPMC composites.

3.3. ATR–FTIR Spectroscopy

The properties of composite materials greatly affect the intermolecular interactions between various components [35,36]. The modulation properties can be enhanced by adjusting intra- and intermolecular interactions between the components [37]. The conventional way of observing the intermolecular interactions involves the use of vibrational spectroscopy [36,38]. However, FTIR spectroscopy provides a quick and straightforward analysis to observe the interaction [39]. Surface functional groups of the composite films were examined to evaluate whether the MoS_2 particles modulate bonding between the additive and matrix before and after particle addition. Angles of incidence greater than the critical angle result in continuous total reflectance of an infrared beam between the sample surface and the ATR crystal. This internal reflectance creates an evanescent wave that the sample may absorb. The infrared beam spectrum, in which the energy is attenuated after multiple reflections, may then be used to analyze the molecular vibrations on the sample surface. The FTIR spectra of the HPMC and MoS_2/HPMC composite films are shown in Figure 6. With the appropriate quantity of MoS_2 additive, minor changes were observed in the intermolecular H bonding and OH bonding (3600–3200 cm^{-1}) of pure HPMC, which indicated that the addition of MoS_2 particles did not reduce the number of molecular bonds. A new band was observed at 690 cm^{-1} (indicated by a dashed line) after the addition of MoS_2 to the matrix owing to the interaction of S^{2-} with H^+ in HPMC. MoS_2 bonded with HPMC and formed molybdenum oxides. The peak at 690 cm^{-1} indicates the formation of MoO_2 (MoS_2 oxidized by water) bonding between HPMC and MoS_2. Based on the change in molecular bonding, an appropriate addition of MoS_2 particles (1 wt%) increases the bonding between additive particles and the HPMC matrix, thus enhancing the mechanical properties of the composite films. The MoS_2 additives used in this study have large particle sizes (at the μm level), and longer-chain HPMC (HPMC 615) may establish more bonding with additives, resulting in higher tensile strength, as demonstrated in Figures 2–5.
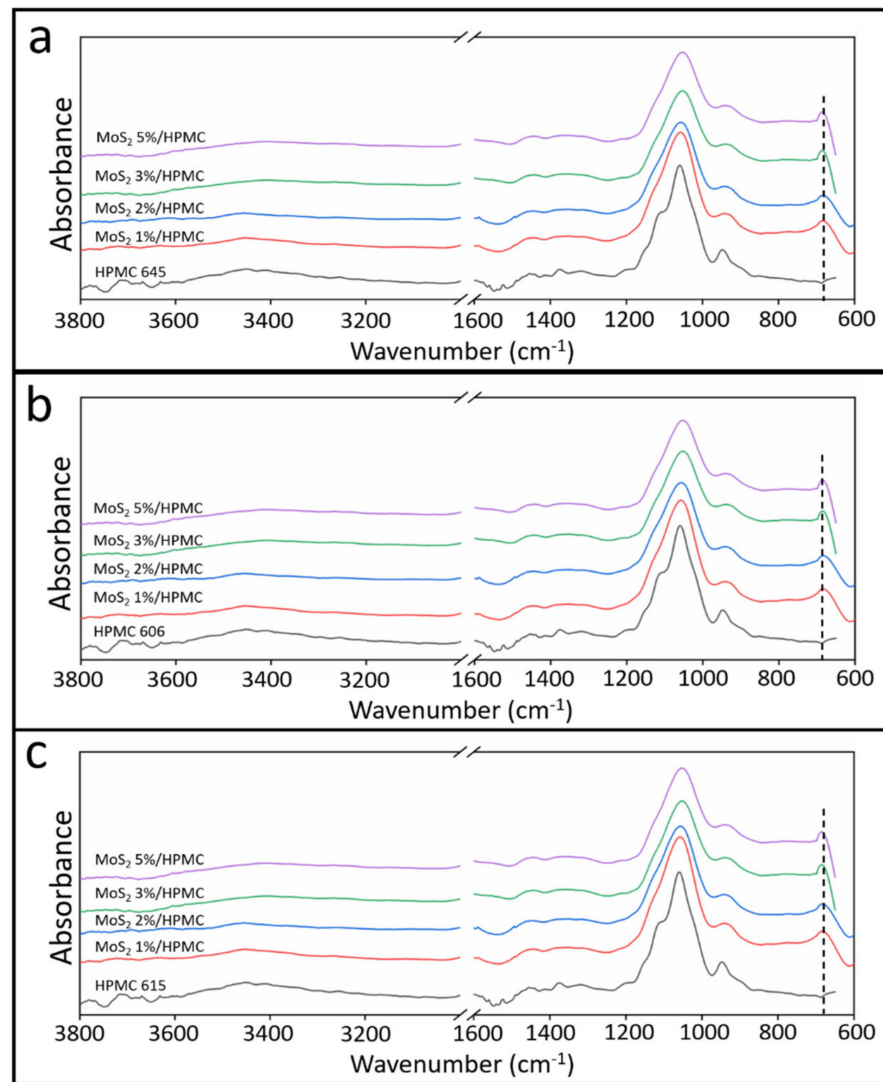
Figure 6. Fourier transform infrared (FTIR) spectra of hydroxypropyl methylcellulose (HPMC): (**a**) 645 composites; (**b**) 606 composites; and (**c**) 615 composites.

3.4. WVP Analysis

The significant index (lower values are preferred) for industrial food packaging is the WVP index [8,40]. As MoS_2 is hydrophobic [11], we predicted that the WVP of the composite films would be reduced. The WVP values of pure HPMC and composite films are shown in Figure 7. The WVP of HPMC films decreased with additives and eventually stabilized beyond a certain level of addition. This demonstrates that the addition of MoS_2 particles effectively reduces WVP. However, without the addition of a dispersant, WVP eventually reached a limit (approximately $1.9 \pm 10\%$ g·mm/kPa·h·m^2 in this study). A small amount of MoS_2 additives can succeed in blocking water vapor from entering the composite material due to the intermolecular bonding between the additive and matrix. It is also helpful to reduce the frictional resistance caused by water vapor.
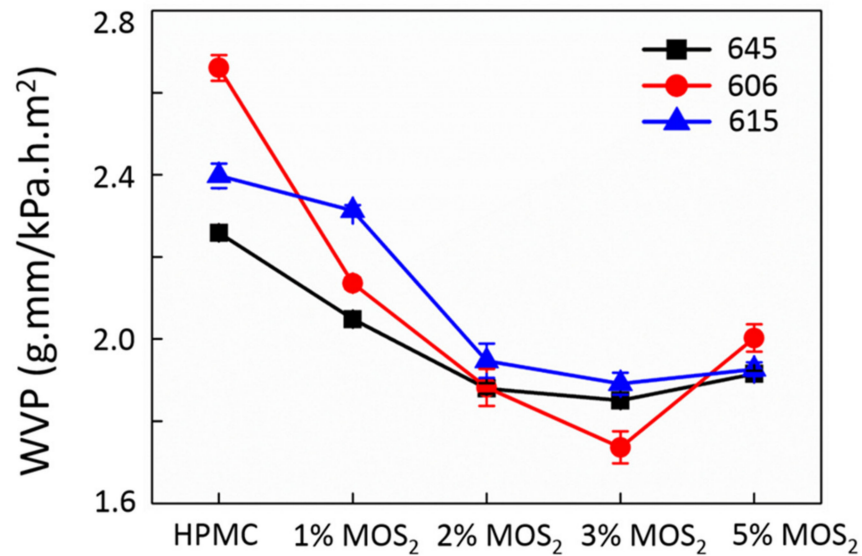
Figure 7. WVP of MoS$_2$/HPMC composites.

3.5. Tribological Behavior of MoS$_2$/HPMC Composites

The MoS$_2$/HPMC 615 composite film offered the best mechanical properties and was used for subsequent wear tests. As shown in Figure 8, the MoS$_2$ additives effectively reduced the friction coefficient by 70%. However, the wear volume hardly reduced. This is in agreement with the study conducted by Shi [17]. The MoS$_2$ additive can facilitate the formation of a transfer layer, thereby reducing the coefficient of friction. MoS$_2$ with a layered structure caused delamination during abrasion and detached itself from the bonded matrix, resulting in wear. A small amount of wear reduction occurred when MoS$_2$ was bonded to the matrix, which led to better load resistance. The deformation of the film surface reduced, and the wear contact area and abrasion volume were lessened. However, the effect of MoS$_2$ additives in reducing the wear of the composite film was not apparent.
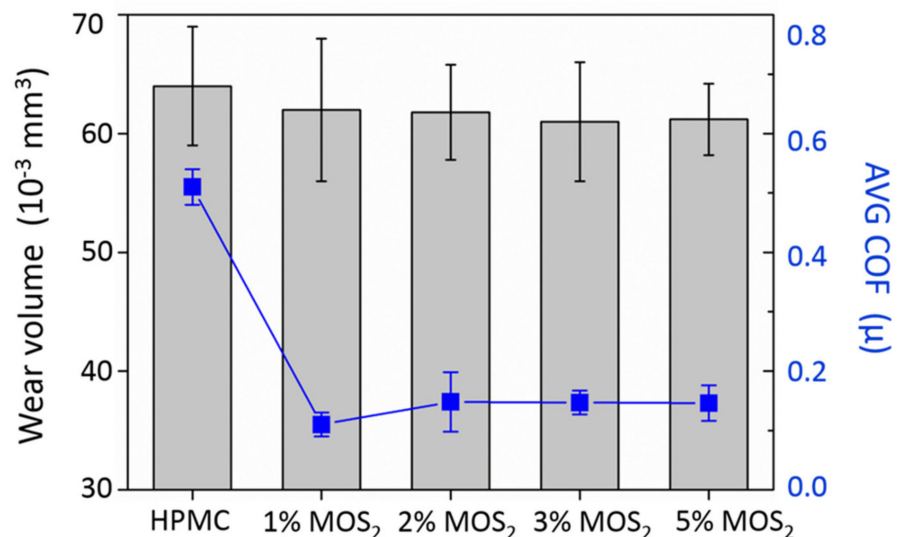

Figure 8. Wear volume and average coefficient of friction of MoS$_2$/HPMC composites.

3.6. Third-Body Tribological Mechanism

A previous study had reported that the addition of MoS$_2$ results in a transfer layer during abrasion, which can effectively reduce the coefficient of friction [29]. However, the generation of the transfer layer did not fully respond to the slight wear reduction and

low coefficient of friction with the MoS_2 additive. The third-body theory can explain this behavior adequately. With the addition of 1 wt% MoS_2 additives, UTS increased by 20% and the elastic modulus increased by 1500%, indicating that MoS_2/HPMC composites are very strong and rigid. When the composite material was subjected to a force, its deformation resistance increased and it provided a better S5M1 (S5 represents the MoS_2/HPMC composite film; M1 represents the elastic deformation) third-body velocity accommodation mechanism, and a better coefficient of friction was obtained. The main reason for transfer layer formation is the delamination of MoS_2 [17]; the presence of MoS_2 in the composite can provide transfer layer formation. In addition, this behavior explains why the coefficient of friction was practically constant with the addition of MoS_2 in composites. The additives simultaneously increased the load resistance of the composite material and the embrittlement of the coating. Embrittlement coating was more likely to abrade out of the system by a third-body flow during abrasion, resulting in wear [29]. These two mechanisms culminated in a slight wear reduction.

4. Conclusions

MoS_2/HPMC composite films were successfully prepared using the solvent evaporation method. The mechanical properties, such as the UTS and Young's modulus, were enhanced dramatically with 1 wt% additive. The addition of MoS_2 to HPMC strengthened the mechanical and vapor barrier behavior of the HPMC composite because of high interfacial bonding between MoS_2 and the HPMC matrix. A matrix with a large molecular weight provided more sites for bonding with additives, thus improving the mechanical properties and load resistance. However, embrittlement of the composite film promoted the separation of MoS_2/HPMC composite material from the film surface, which formed an effective transfer/protection layer and resulted in excellent tribological properties. The properties of HPMC were enhanced when the additives were incorporated. Although FTIR spectra illustrate that intermolecular forces transpire between additive and matrix materials, results from other analytical instruments is essential. The principal components analysis-assisted ATR–FTIR and thermogravimetric analysis can provide additional evidence to make the findings more significant. The application of environmentally friendly materials with improved mechanical properties would be beneficial for the food packaging industry.

Author Contributions: Conceptualization, S.-C.S.; methodology, S.-C.S. and P.K.M.; validation, S.-C.S. and P.K.M.; formal analysis, S.-C.S. and P.K.M.; investigation, S.-C.S., P.K.M., and T.-H.C.; resources, S.-C.S. and T.-H.C.; data curation, P.K.M.; writing—original draft preparation, S.-C.S., and P.K.M.; writing—review and editing, S.-C.S.; visualization, S.-C.S.; supervision, S.-C.S. and T.-H.C.; project administration, S.-C.S., and T.-H.C.; funding acquisition, T.-H.C. All authors have read and agreed to the published version of the manuscript.

Institutional Review Board Statement: Not applicable.

Informed Consent Statement: Not applicable.

Conflicts of Interest: The authors declare no conflict of interest.

References

1. Alfei, S.; Marengo, B.; Zuccari, G. Nanotechnology application in food packaging: A plethora of opportunities versus pending risks assessment and public concerns. *Food Res. Int.* **2020**, 109664. [CrossRef]
2. Alfei, S.; Schito, A.M.; Zuccari, G. Biodegradable and compostable shopping bags under investigation by ftir spectroscopy. *Appl. Sci.* **2021**, *11*, 621. [CrossRef]
3. Mohammadi, M.A.; Ramezani, S.; Hosseini, H.; Mortazavian, A.M.; Hosseini, S.M.; Ghorbani, M. Electrospun antibacterial and antioxidant zein/polylactic acid/hydroxypropyl methylcellulose nanofibers as an active food packaging system. *Food Bioproc. Tech.* **2021**, 1–13. [CrossRef]

4. Chaiwarit, T.; Kantrong, N.; Sommano, S.R.; Rachtanapun, P.; Junmahasathien, T.; Kumpugdee-Vollrath, M.; Jantrawut, P. Extraction of tropical fruit peels and development of hpmc film containing the extracts as an active antibacterial packaging material. *Molecules* **2021**, *26*, 2265. [CrossRef] [PubMed]

5. Di Filippo, M.F.; Dolci, L.S.; Liccardo, L.; Bigi, A.; Bonvicini, F.; Gentilomi, G.A.; Passerini, N.; Panzavolta, S.; Albertini, B. Cellulose derivatives-snail slime films: New disposable eco-friendly materials for food packaging. *Food Hydrocoll.* **2021**, *111*, 106247. [CrossRef]

6. Priyadarshi, R.; Rhim, J.-W. Chitosan-based biodegradable functional films for food packaging applications. *Innov. Food Sci. Emerg. Technol.* **2020**, *62*, 102346. [CrossRef]

7. Kumar, S.; Mukherjee, A.; Dutta, J. Chitosan based nanocomposite films and coatings: Emerging antimicrobial food packaging alternatives. *Trends Food Sci. Technol.* **2020**, *97*, 196–209. [CrossRef]

8. Yadav, S.; Mehrotra, G.; Dutta, P. Chitosan based zno nanoparticles loaded gallic-acid films for active food packaging. *Food Chem.* **2021**, *334*, 127605. [CrossRef]

9. Strachan, J. Solubility of cellulose in water. *Nature* **1938**, *141*, 332–333. [CrossRef]

10. Shi, S.-C.; Jiang, S.-Z. Influence of graphene/copper hybrid nanoparticle additives on tribological properties of solid cellulose lubricants. *Surf. Coat. Technol.* **2020**, *389*, 125655. [CrossRef]

11. Shi, S.-C.; Huang, T.-F. Self-healing materials for ecotribology. *Materials* **2017**, *10*, 91. [CrossRef] [PubMed]

12. Nosonovsky, M.; Bhushan, B. *Green Tribology: Biomimetics, Energy Conservation and Sustainability*, 1st ed.; Michael, N., Bharat, B., Eds.; Springer: Berlin, Germany, 2012; Volume 1, pp. 79–104.

13. Fahs, A.; Brogly, M.; Bistac, S.; Schmitt, M. Hydroxypropyl methylcellulose (hpmc) formulated films: Relevance to adhesion and friction surface properties. *Carbohydr. Polym.* **2010**, *80*, 105–114. [CrossRef]

14. Pei, Y.; Ocelik, V.; De Hosson, J.T.M. Sicp/ti6al4v functionally graded materials produced by laser melt injection. *Acta Mater.* **2002**, *50*, 2035–2051. [CrossRef]

15. Shi, S.-C.; Su, C.-C. Electrochemical behavior of hydroxypropyl methylcellulose acetate succinate as novel biopolymeric anticorrosion coating. *Mater. Chem. Phys.* **2020**, *248*, 122929. [CrossRef]

16. Liu, M.; Zhu, H.; Wang, Y.; Sevencan, C.; Li, B.L. Functionalized mos2-based nanomaterials for cancer phototherapy and other biomedical applications. *ACS Mater. Lett.* **2021**, *3*, 462–496. [CrossRef]

17. Shi, S.-C.; Wu, J.-Y.; Peng, Y.-Q. Transfer layer formation in mos2/hydroxypropyl methylcellulose composite. *Wear* **2018**, *408*, 208–213. [CrossRef]

18. Wrona, M.; Cran, M.J.; Nerín, C.; Bigger, S.W. Development and characterisation of hpmc films containing pla nanoparticles loaded with green tea extract for food packaging applications. *Carbohydr. Polym.* **2017**, *156*, 108–117. [CrossRef]

19. Shi, S.-C.; Peng, Y.-Q. Preparation and tribological studies of stearic acid-modified biopolymer coating. *Prog. Org. Coat.* **2020**, *138*, 105304. [CrossRef]

20. Tagami, T.; Ito, E.; Kida, R.; Hirose, K.; Noda, T.; Ozeki, T. 3d printing of gummy drug formulations composed of gelatin and an hpmc-based hydrogel for pediatric use. *Int. J. Pharm.* **2021**, *594*, 120118. [CrossRef] [PubMed]

21. Yu, J.Y.; Kim, J.A.; Joung, H.J.; Ko, J.A.; Park, H.J. Preparation and characterization of curcumin solid dispersion using hpmc. *J. Food Sci.* **2020**, *85*, 3866–3873. [CrossRef]

22. Malik, G.K.; Mitra, J. Zinc oxide nanoparticle synthesis, characterization, and their effect on mechanical, barrier, and optical properties of hpmc-based edible film. *Food BioProc. Tech.* **2021**, *14*, 441–456. [CrossRef]

23. Shi, S.-C.; Lu, F.-I. Biopolymer green lubricant for sustainable manufacturing. *Materials* **2016**, *9*, 338. [CrossRef]

24. Xu, R.; Wei, N.; Li, Z.; Song, X.; Li, Q.; Sun, K.; Yang, E.; Gong, L.; Sui, Y.; Tian, J. Construction of hierarchical 2d/2d ti3c2/mos2 nanocomposites for high-efficiency solar steam generation. *J. Colloid. Interface Sci.* **2021**, *584*, 125–133. [CrossRef]

25. He, D.; Yang, Y.; Zhou, Y.; Wan, J.; Wang, H.; Fan, X.; Li, Q.; Huang, H. Electricity generation from phase-engineered flexible mos2 nanosheets under moisture. *Nano Energy* **2021**, *81*, 105630. [CrossRef]

26. Subad, R.A.; Akash, T.S.; Bose, P.; Islam, M.M. Engineered defects to modulate fracture strength of single layer mos2: An atomistic study. *Physica B Condens. Matter* **2020**, *592*, 412219. [CrossRef]

27. Shi, S.-C.; Wu, J.-Y.; Huang, T.-F.; Peng, Y.-Q. Improving the tribological performance of biopolymer coating with mos 2 additive. *Surf. Coat. Technol.* **2016**, *303*, 250–255. [CrossRef]

28. Nomura, T.; Moriguchi, H.; Tsuda, K.; Isobe, K.; Ikegaya, A.; Moriyama, K. Material design method for the functionally graded cemented carbide tool. *Int. J. Refract. Hard Mater.* **1999**, *17*, 397–404. [CrossRef]

29. Godet, M. Third-bodies in tribology. *Wear* **1990**, *136*, 29–45. [CrossRef]

30. Godet, M. The third-body approach: A mechanical view of wear. *Wear* **1984**, *100*, 437–452. [CrossRef]

31. Shi, S.-C.; Pek, S.-S. Third-body and dissipation energy in green tribology film. *Appl. Sci.* **2019**, *9*, 3787. [CrossRef]

32. Panitz, J.; Pope, L.; Lyons, J.; Staley, D. The tribological properties of mos2 coatings in vacuum, low relative humidity, and high relative humidity environments. *J. Vac. Sci. Technol. A* **1988**, *6*, 1166–1170. [CrossRef]

33. Hilton, M.R.; Bauer, R.; Didziulis, S.V.; Dugger, M.T.; Keem, J.M.; Scholhamer, J. Structural and tribological studies of mos2 solid lubricant films having tailored metal-multilayer nanostructures. *Surf. Coat. Technol.* **1992**, *53*, 13–23. [CrossRef]

34. Descartes, S.; Berthier, Y. Rheology and flows of solid third bodies: Background and application to an mos 1.6 coating. *Wear* **2002**, *252*, 546–556. [CrossRef]

35. Yamada, K.; Mitsutake, T.; Takayanagi, M.; Kajiyama, T. Mechanical properties and intermolecular interactions in molecular composites composed of wholly aromatic polyamide and poly-(amide-imide). *J. Macromol. Sci. Chem. A.* **1989**, *26*, 891–902. [CrossRef]

36. Wang, H.; Tashiro, K. Reinvestigation of crystal structure and intermolecular interactions of biodegradable poly (3-hydroxybutyrate) α-form and the prediction of its mechanical property. *Macromolecules* **2016**, *49*, 581–594. [CrossRef]

37. Galant, O.; Bae, S.; Silberstein, M.N.; Diesendruck, C.E. Highly stretchable polymers: Mechanical properties improvement by balancing intra-and intermolecular interactions. *Adv. Funct. Mater.* **2020**, *30*, 1901806. [CrossRef]

38. Baiz, C.R.; Błasiak, B.; Bredenbeck, J.; Cho, M.; Choi, J.-H.; Corcelli, S.A.; Dijkstra, A.G.; Feng, C.-J.; Garrett-Roe, S.; Ge, N.-H. Vibrational spectroscopic map, vibrational spectroscopy, and intermolecular interaction. *Chem. Rev.* **2020**, *120*, 7152–7218. [CrossRef]

39. Chen, Z.; Mo, X.; He, C.; Wang, H. Intermolecular interactions in electrospun collagen–chitosan complex nanofibers. *Carbohydr. Polym.* **2008**, *72*, 410–418. [CrossRef]

40. Goudarzi, V.; Shahabi-Ghahfarrokhi, I.; Babaei-Ghazvini, A. Preparation of ecofriendly uv-protective food packaging material by starch/tio2 bio-nanocomposite: Characterization. *Int. J. Biol. Macromol.* **2017**, *95*, 306–313. [CrossRef]